

On the computation of space-time correlations by large-eddy simulation

By Guo-Wei He[†], Meng Wang AND Sanjiva K. Lele

1. Motivation and objectives

Sound radiated by turbulent flow is dependent on the space-time characteristics of the flow field. According to Lighthill's theory (Lighthill 1952; Proudman 1952), acoustic power spectra in the far-fields are determined by the two-time, two-point Eulerian velocity correlations. This has significant implications to the use of large eddy simulation (LES) for aerodynamic noise prediction. The existing subgrid scale (SGS) models are mostly constructed to predict spatial statistics such as energy spectra (Meneveau & Katz 2000). However, it is not clear whether these models can lead to accurate space-time correlations, or frequency contents at individual wavenumbers. The latter information is essential to accurate noise predictions, because for a given frequency, only the spectral element of the source field corresponding to the acoustic wavenumber in a given direction can radiate in that direction (Crighton 1975). This represents a very small fraction of flow energy, and is very susceptible to numerical and modeling errors. Hence, accurate prediction of the space-time correlation is a new requirement imposed on SGS modeling by aeroacoustic applications.

For brevity, we henceforth refer to the two-time, two-point correlation of the velocity field simply as time correlation. It describes the space-time statistics of turbulent flows. The time correlation can be equivalently expressed by a two-time correlation of velocity Fourier modes in spectral space

$$C(k, \tau) = \langle u_i(\mathbf{k}, t) u_i(-\mathbf{k}, t + \tau) \rangle, \quad (1.1)$$

or its normalized form

$$R(k, \tau) = \frac{\langle u_i(\mathbf{k}, t) u_i(-\mathbf{k}, t + \tau) \rangle}{\langle u_i(\mathbf{k}, t) u_i(-\mathbf{k}, t) \rangle}. \quad (1.2)$$

Previous research (He, Rubinstein & Wang 2002) compared the normalized time correlations or correlation coefficients in forced isotropic turbulence calculated by direct numerical simulation (DNS) and LES using a standard spectral eddy viscosity model (Chollet & Lesieur 1981). The comparisons show that the LES overpredicts decorrelation time scales. A following-up study (He, Wang & Lele 2002) made the comparisons in decaying turbulence, using the classic Smagorinsky model (Smagorinsky 1963), the dynamic Smagorinsky model (Germano et al. 1991) and the multiscale LES method (Hughes, Mazzei & Oberai 2001). The overpredictions are still observed. These numerical observations motivated the present analysis to investigate the overpredictions and their influence on sound power spectra. The analysis will be carried out for the un-

[†] Permanent address: LNM, Institute of Mechanics, Chinese Academy of Sciences, Beijing, 100080, China; Email: hgw@lnm.imech.ac.cn

normalized time correlations, not the normalized ones as before, since the former are the ones actually used in the computation of sound power spectra.

The analysis starts with a generalization of Kraichnan's sweeping hypothesis (Kraichnan 1964) from stationary turbulence to decaying turbulence. This involves replacing a constant convection velocity by a time-dependent one in a simple kinematic model. The solution of the kinematic model defines a time-dependent sweeping velocity. Kraichnan's sweeping hypothesis is the foundation of the turbulence theory on time correlation. Kaneda and Gotoh (1991) and Kaneda (1993) developed the Lagrangian renormalization group theory and the Taylor expansion technique for time correlations. Rubinstein and Zhou (2000) used the sweeping hypothesis to formulate the scaling law of sound power spectra.

The present analysis on time correlations will shed some light on the ability of LES to predict sound power spectra, since the latter can be analytically expressed as an integration of time correlations using the quasi-normal closure assumption. Previous evaluations (e. g. Witkowska, Juvé & Brasseur 1997; Seror et al. 2001) are made directly on acoustic fields. These calculations unavoidably have to cope with the numerical errors caused by the truncation of the source region (Crighton 1993; Wang, Lele & Moin 1996). Instead, we will discuss the influences of the SGS modeling on the accuracy of sound prediction through an analysis of time correlations.

In this paper, we consider decaying homogeneous isotropic turbulence. Unlike stationary turbulence, the time correlations in decaying turbulence are dependent on both time separations and starting time. Therefore, two different starting time will be chosen, one at the energy propagation stage and another at the final decaying stage.

2. Main results

2.1. Numerical results

A decaying homogeneous isotropic turbulence in a cubic box of side 2π is simulated by DNS with grid size 256^3 and LES with grid size 64^3 . A standard pseudo-spectral method is used, in which spatial differentiation is made by the Fourier spectral method, time advancement is made by a second-order Adams-Bashforth method with the same time steps for both DNS and LES, and molecular viscous effects are accounted for by an exponential integrating factor. All nonlinear terms are dealiased with the two-thirds rule.

The following SGS models are used in the LES:

(1) The spectral eddy viscosity model: we use the Chollet-Lesieur standard form for the spectral eddy viscosity (Chollet & Lesieur 1981), where the cutoff energy is evaluated from the LES.

(2) The Smagorinsky model (Smagorinsky 1963): the Smagorinsky constant is $C_s = 0.22$ and the filter width is set equal to the inverse of the largest effective wave number $k_c = 21$.

(3) The dynamic Smagorinsky model (Germano et al. 1991): the Smagorinsky coefficients are determined by the Germano identity. The grid filter width is k_c^{-1} and the test filter width is taken as $2k_c^{-1}$.

(4) The multi-scale LES method (Hughes et al. 2001): we decompose the filtered Navier-Stokes equations into the large scale equations for the lower one-half Fourier modes and the small scale equations for the remaining half Fourier modes. The dynamic Smagorinsky model is only applied to the small scale equations.

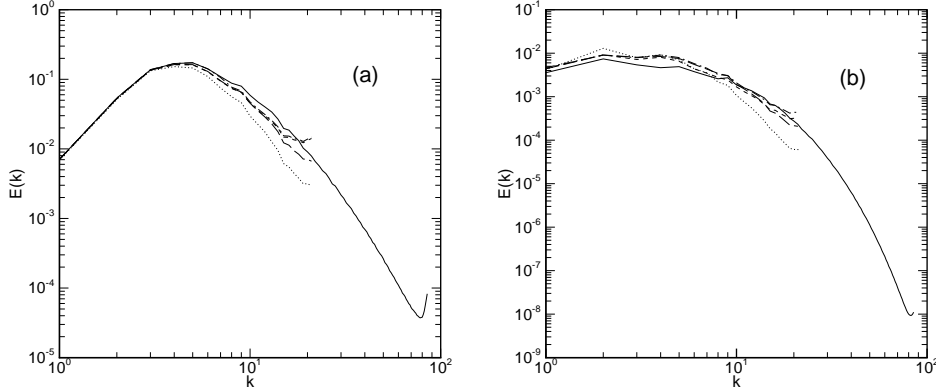


FIGURE 1. Energy spectra at (a) $t = 0.5$ and (b) $t = 4.0$ — DNS; ---- dynamic Smagorinsky model; ——— multiscale LES; ····· Smagorinsky model; -·-·- spectral eddy viscosity model.

The initial condition for DNS is an isotropic Gaussian field with energy spectrum

$$E(k, 0) \propto (k/k_0)^4 \exp[-2(k/k_0)^2], \quad (2.1)$$

where $k_0 = 4.68$ is the wave number corresponding to the peak of the energy spectrum. The shape of the energy spectrum excludes the effects of the box size. The initial Reynolds number based on Taylor's microscale is 127.4. The initial condition for LES is obtained by filtering the initial DNS velocity fields with filtering wavenumber $k_c = 64/3 \approx 21$. Therefore, the initial LES and filtered DNS velocity fields are exactly the same. At early stages, the LES and DNS velocity fields are highly correlated due to the same initial conditions. Therefore, the time correlations of the LES velocity field are nearly the same as those of the DNS field. As time progresses, the LES fields become decorrelated from the DNS fields. The difference in time correlations between the LES and DNS velocity fields are then observed. Therefore, we first advanced the DNS and LES velocities in time to decorrelate them before starting to calculate the time correlations.

The energy spectra at $t = 0.5$ and $t = 4.0$ are presented in Fig. 1. Generally speaking, the LES results are in good agreement with the DNS result at small wavenumbers but drop faster than DNS at large wavenumbers. The decay of the total resolved energy is presented in Fig. 2. The results from LES with all SGS models follow the DNS results with some deviations throughout the entire time range. They exhibit excessive dissipation before the time $t = 1.5$ (the energy propagation range) and insufficient dissipations after $t = 1.5$ (the final decay range). Note that $t = 0$ does not correspond to the start time of the simulation. Rather, it is 0.1 time units after the start, and hence the deviations among DNS and LES results are already significant. In both Figs. 1 and 2, the multiscale LES results are the best of all models and the classic Smagorinsky model results are the worst. The dynamic Smagorinsky model and spectral eddy viscosity model yield results in the middle with small differences.

Figure 3 plots the un-normalized time correlations of the velocity fields from the DNS and LES for wavenumbers $k = 5, 9, 13,$ and 17 , spanning a range of scales from the integral scale to the lower end of the resolved scale. The starting time is $t = 0.5$. It clearly shows that there exist discrepancies between the LES and DNS results, and that the discrepancies become larger with increasing wavenumbers. Again, the classic Smagorinsky

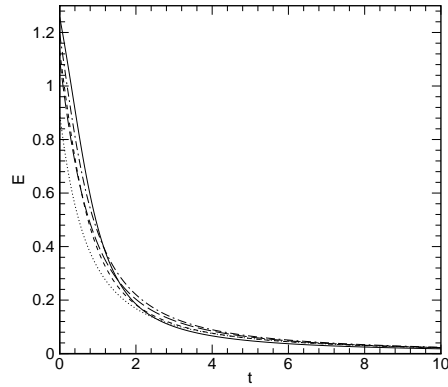


FIGURE 2. Decay of total resolved energy. — DNS; - - - dynamic Smagorinsky model; - · - multiscale LES; ····· Smagorinsky model; - - - spectral eddy viscosity model.

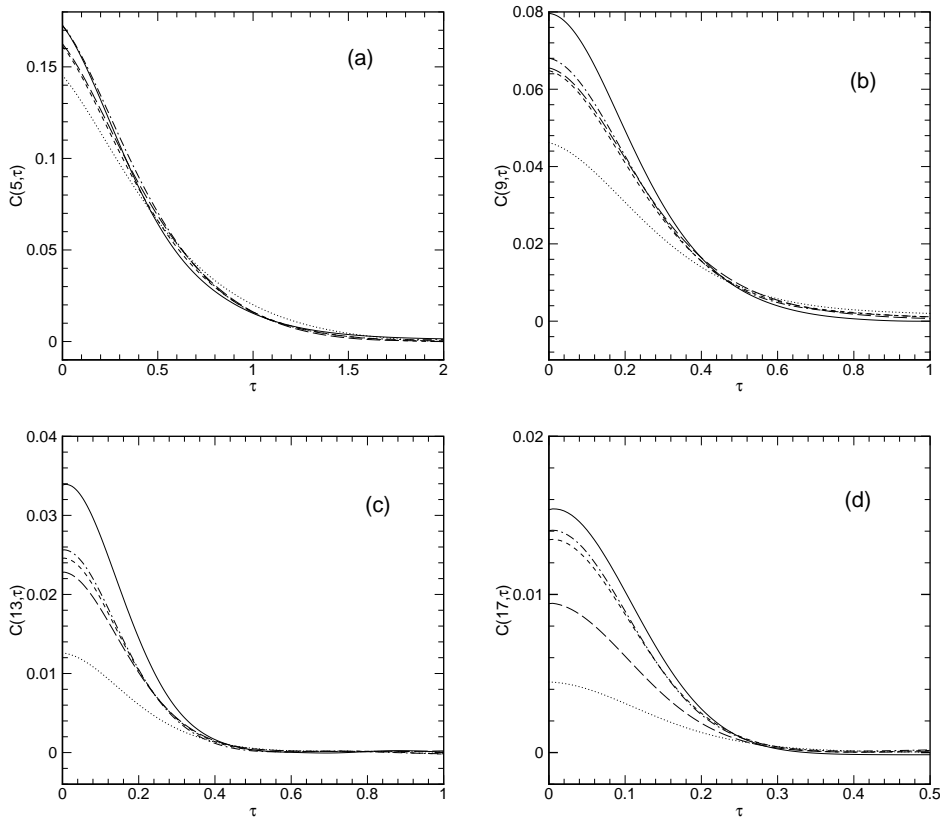


FIGURE 3. Time correlation $C(k, \tau)$ vs time lag τ with starting time $t = 0.5$ for (a) $k = 5$, (b) $k = 9$, (c) $k = 13$, (d) $k = 17$. — DNS; - - - dynamic Smagorinsky model; - · - multiscale LES; ····· Smagorinsky model; - - - spectral eddy viscosity model.

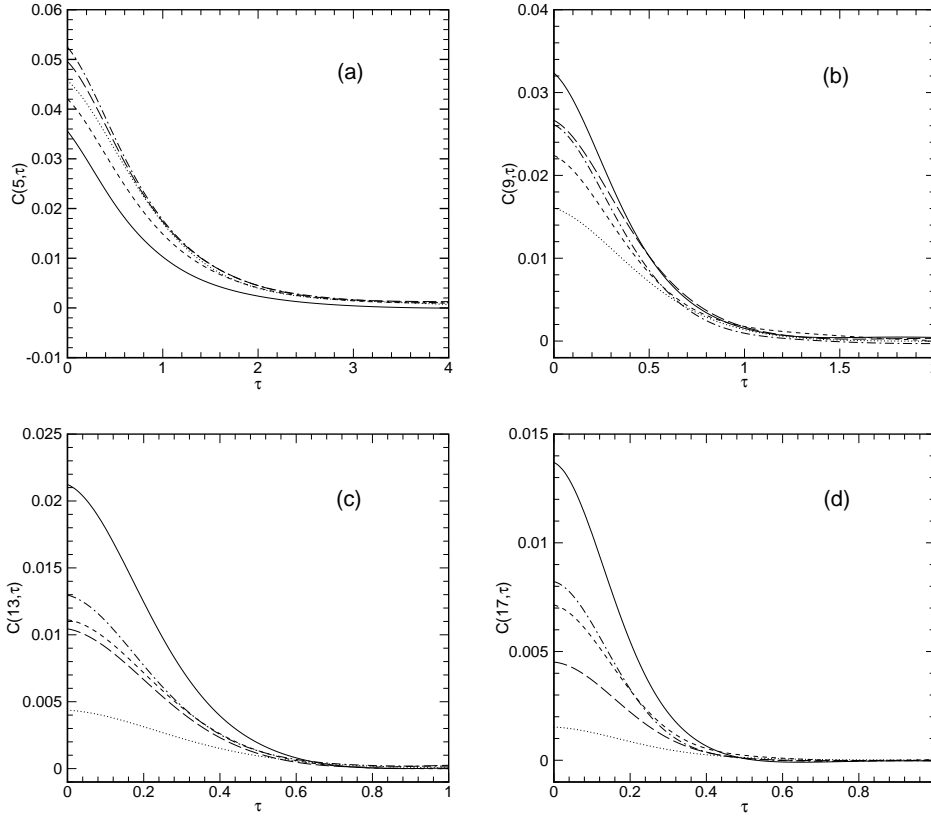


FIGURE 4. Time correlation $C(k, \tau)$ vs time lag τ with starting time $t = 1.5$ for (a) $k = 5$, (b) $k = 9$, (c) $k = 13$, (d) $k = 17$. — DNS; ---- dynamic Smagorinsky model; —·— multiscale LES; ····· Smagorinsky model; - - - spectral eddy viscosity model.

model results are the least accurate of all models, the multiscale LES method is the most accurate, and the spectral eddy viscosity model and the dynamic Smagorinsky model lie in between, the latter being slightly better than the former.

Figure 4 plots the same time correlations as in Fig. 3 but with a different starting time $t = 1.5$. The discrepancies observed are qualitatively the same as in the $t = 0.5$ case, which indicates that the SGS modeling errors equally affect the time correlations in the final decay range.

In summary, it is observed in decaying isotropic turbulence that discrepancies exist between the un-normalized time correlations calculated from DNS and those from the LES. These discrepancies will be analysed in the next section.

2.2. Analysis of the numerical results

The analysis is based on the generalized sweeping hypothesis for decaying turbulence. In the sweeping hypothesis for stationary isotropic turbulence, the convection velocity is constant (Kraichnan 1964). However, in decaying turbulence, the convection velocity varies with time. A generalization can be made by introducing a time-dependent convection velocity, which evolves slowly relative to the time scales of velocity fluctuations.

Consider a fluctuating velocity Fourier mode $\mathbf{u}(\mathbf{k}, t)$ convected by a bulk velocity $\mathbf{v}(t)$. We assume that the wavenumbers \mathbf{k} of the fluctuating velocity are sufficiently large. The flow scales associated with these wavenumbers are small, over which the convection velocity is spatially uniform and relatively large in magnitudes. In this case, the convection effect is dominant. The governing equation for the fluctuating velocity modes is therefore

$$\frac{\partial \mathbf{u}(\mathbf{k}, t)}{\partial t} + i[\mathbf{k} \cdot \mathbf{v}(t)]\mathbf{u}(\mathbf{k}, t) = 0, \quad (2.2)$$

which yields

$$\mathbf{u}(\mathbf{k}, t + \tau) = \mathbf{u}(\mathbf{k}, t) \exp\left(-i \int_t^{t+\tau} \mathbf{k} \cdot \mathbf{v}(s) ds\right). \quad (2.3)$$

Then, the time correlation can be expressed by

$$\begin{aligned} & \langle \mathbf{u}(\mathbf{k}, t + \tau) \mathbf{u}(-\mathbf{k}, t) \rangle \\ &= \langle \mathbf{u}(\mathbf{k}, t) \mathbf{u}(-\mathbf{k}, t) \rangle \exp\left(-\frac{1}{2} k^2 \int_t^{t+\tau} \int_t^{t+\tau} \langle \mathbf{v}(s') \mathbf{v}(s'') \rangle ds' ds''\right). \end{aligned} \quad (2.4)$$

In the derivation of (2.4), the convection velocity $\mathbf{v}(t)$ is assumed to be Gaussian and independent of the velocity $\mathbf{u}(\mathbf{x}, t)$ at the starting time t . These assumptions can be justified by the near-Gaussianity of the large-scale velocity and its initial independence of the small-scale velocity. By introducing a sweeping velocity

$$V^2(t, \tau) = \frac{1}{\tau^2} \int_t^{t+\tau} \int_t^{t+\tau} \langle \mathbf{v}(s') \mathbf{v}(s'') \rangle ds' ds'', \quad (2.5)$$

we obtain a general expression of time correlation similar to the one in stationary turbulence

$$\langle \mathbf{u}(\mathbf{k}, t + \tau) \mathbf{u}(-\mathbf{k}, t) \rangle = \langle \mathbf{u}(\mathbf{k}, t) \mathbf{u}(-\mathbf{k}, t) \rangle \exp\left(-\frac{1}{2} k^2 V^2(t, \tau) \tau^2\right). \quad (2.6)$$

The calculation of the sweeping velocity (2.5) can be further simplified by assuming the following form of the bulk velocity correlation

$$\langle \mathbf{v}(s') \mathbf{v}(s'') \rangle = \langle \mathbf{v}^2(s') \rangle \exp\left(-\lambda |s' - s''|\right), \quad (2.7)$$

where λ^{-1} is a correlation time scale. Substituting (2.7) into (2.5), we find

$$V^2(t, \tau) = \frac{1}{\tau^2} \int_t^{t+\tau} \langle \mathbf{v}^2(s') \rangle \lambda^{-1} \left(2 - \exp[-\lambda(s' - t)] - \exp[-\lambda(t + \tau - s')]\right) ds'. \quad (2.8)$$

In isotropic turbulence, the bulk velocity is determined by large scale motions. Hence, its decorrelation time scale λ^{-1} is much larger than those of velocity fluctuation modes considered here. Since the time separation τ of interest is within the decorrelation time scales of the velocity fluctuations, we have $\lambda\tau \ll 1$. Using Taylor series expansion with respect to $\lambda\tau$ and ignoring the second and higher order terms in (2.8), we obtain

$$V^2(t, \tau) = \frac{1}{\tau} \int_t^{t+\tau} \langle \mathbf{v}^2(s') \rangle ds'. \quad (2.9)$$

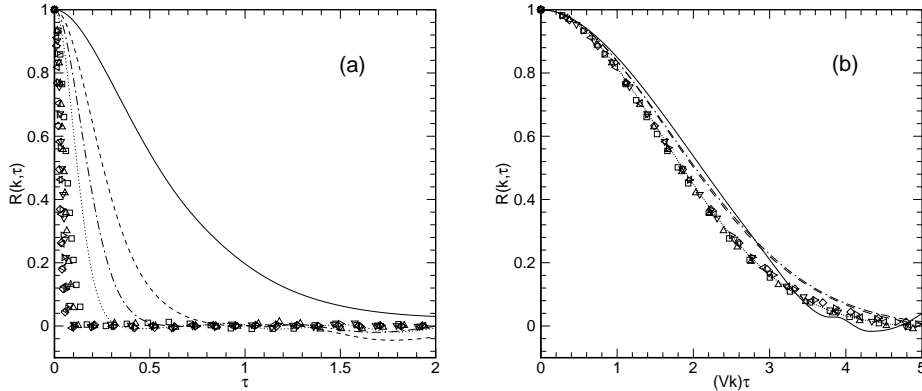


FIGURE 5. Normalized time correlation $R(k, \tau)$ vs (a) un-normalized and (b) normalized time lag for different modes computed using DNS. — $k = 5$; ---- $k = 9$; -·-·- $k = 13$; ····· $k = 17$; □ $k = 30$; △ $k = 40$; ▽ $k = 50$; ▷ $k = 60$; ◁ $k = 70$; ◇ $k = 80$.

Note that the bulk velocity is associated with the energy-containing motions, and its variance $\langle \mathbf{v}^2(t) \rangle$ is the total energy of the instantaneous velocity field. Since the energy decay is relatively small over the decorrelation time scale, the sweeping velocity can be easily calculated by simple approximations $V^2(t, \tau) \cong \langle \mathbf{v}^2(t + \tau) \rangle$ or $V^2(t, \tau) \cong [\langle \mathbf{v}^2(t) \rangle + \langle \mathbf{v}^2(t + \tau) \rangle]/2$. The former is used in the following discussions.

Figure 5 plots the normalized time correlations $R(k, \tau)$ from DNS for wavenumbers $k = 5, 9, 13, 17, 30, 40, 50, 60, 70$ and 80 , where the correlations are normalized by the instantaneous energy spectra. The time separation is un-normalized in Fig. 5(a) and normalized by the scale-dependent similarity variable Vk in Fig. 5(b). The latter figure clearly exhibits that, with time normalization, all curves for different modes collapse. This verifies the validity of the generalized sweeping velocity in decaying turbulence.

Equation (2.6) indicates that the normalized time correlations are solely determined by the sweeping velocities. In the present LES, the sweeping velocities are smaller than that of DNS values because of the reduced total energy. Therefore, the time correlations in LES decay more slowly than the ones in DNS. That is to say, the LES overpredicts the decorrelation time scales compared to DNS. Figure 6 plots the normalized time correlations from the DNS and LES with respect to the un-normalized time for the modes $k = 5, 9, 13, 17$. It confirms that the time correlations from LES decay more slowly than the ones from DNS. Again, the multiscale LES method is the most accurate and the classic Smagorinsky model is the least accurate of the all models tested. The dynamic Smagorinsky model and the spectral eddy viscosity model are in the middle.

Equation (2.6) also indicates that if the time separation is normalized by Vk , the un-normalized time correlations are solely determined by the instantaneous energy spectra. Figure 7 plots the un-normalized correlations vs the normalized time separation. It shows that the LES underestimates the magnitudes of time correlations relative to the DNS results. The underestimation obviously becomes more significant as the wavenumber increases, which is consistent with the more severe drops of the LES energy spectra at high wavenumbers. Again, the relative performance of the SGS models in terms of the magnitudes of time correlations is the same as before.

In conclusion, the discrepancies between the time correlations computed using DNS and LES consist of two parts: the decorrelation time scale and magnitude. The errors in

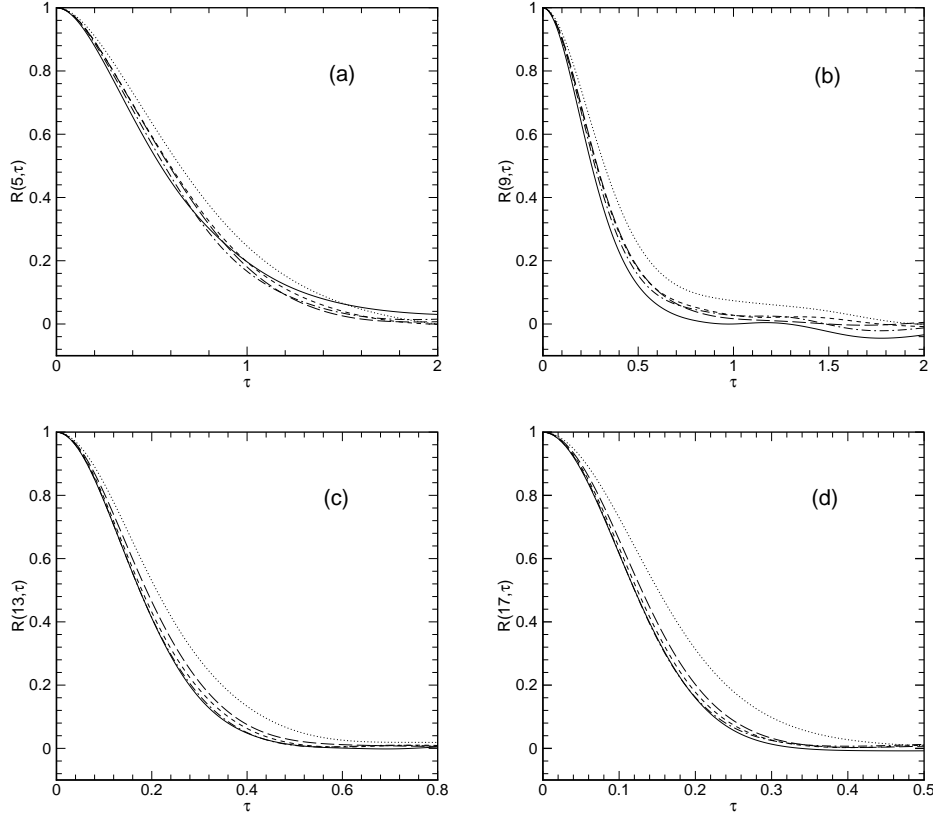


FIGURE 6. Normalized time correlation $R(k, \tau)$ vs time lag τ with starting time $t = 0.5$ for (a) $k = 5$, (b) $k = 9$, (c) $k = 13$, (d) $k = 17$. — DNS; ---- dynamic Smagorinsky model; -·- multiscale LES; ····· Smagorinsky model; - - - spectral eddy viscosity model.

decorrelation scales are induced by the instantaneous sweeping velocity, and the errors in magnitudes are induced by the instantaneous energy spectra. In relative terms, the errors in decorrelation time scales are less significant than those in magnitudes. However, they must not be ignored since the sound power spectra are sensitive to the decorrelation time scale, (see discussions in the next section). Note that the sweeping velocity used in our analysis is the *r.m.s.* of velocity fluctuations, or the square root of the total energy. Thus, an accurate prediction of the instantaneous energy spectra is most critical to the accurate computation of the time correlations.

2.3. Discussion

It is difficult to determine the influence of SGS modeling on acoustic power spectra through numerical evaluation in general, since it involves the truncation of the source region (Wang et al. 1996). To avoid this problem, we use an analytical expression of acoustic power spectra based on Lighthill's theory and the quasi-normal closure assumption. The analytical expression is only valid for stationary turbulence. However, reasonable inferences can be drawn for decaying turbulence through this analysis.

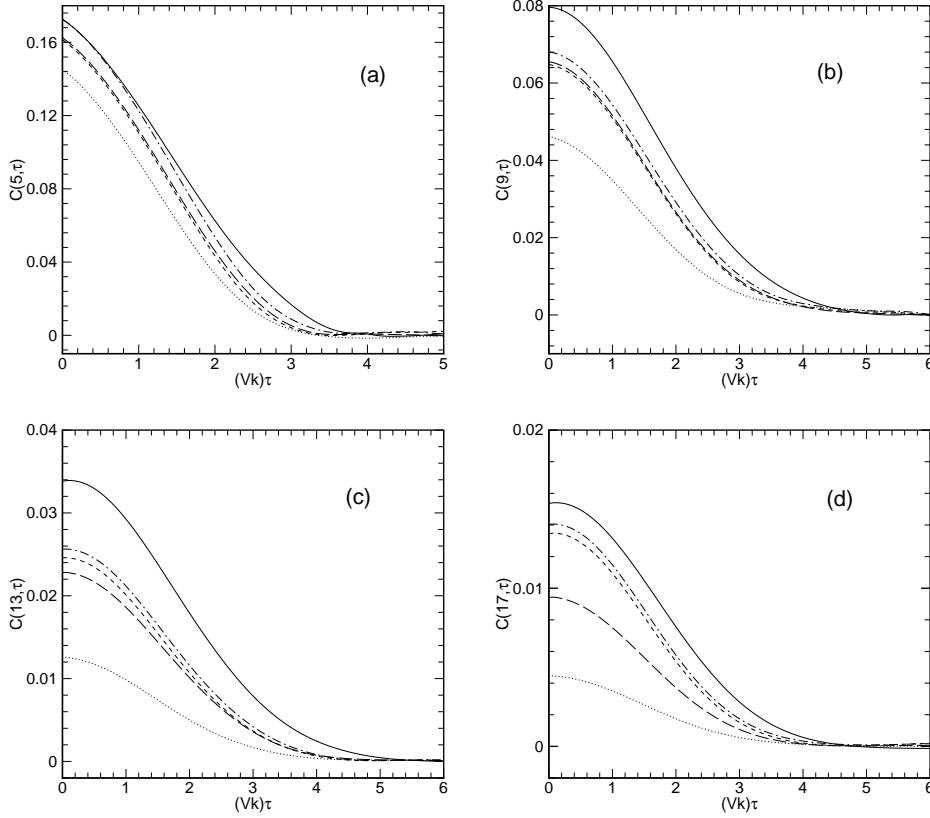


FIGURE 7. Un-normalized time correlation $C(k, \tau)$ vs the normalized time lag τ with starting time $t = 0.5$ for (a) $k = 5$, (b) $k = 9$, (c) $k = 13$, (d) $k = 17$. — DNS; ---- dynamic Smagorinsky model; - · - multiscale LES; ····· Smagorinsky model; - - - spectral eddy viscosity model.

According to Lighthill's theory (Lighthill 1952), the acoustic pressure in a far-field position \mathbf{x} is given by

$$p(\mathbf{x}, t) = \frac{1}{4\pi c^2} \frac{x_i x_j}{|\mathbf{x}|^3} \int_{\Omega} d\mathbf{y} \frac{\partial^2}{\partial t^2} T_{ij} \left(\mathbf{y}, t - \frac{|\mathbf{x} - \mathbf{y}|}{c} \right), \quad (2.10)$$

where $T_{ij}(\mathbf{y}, t) = \rho u_i(\mathbf{y}, t) u_j(\mathbf{y}, t)$ is the Lighthill stress tensor, Ω the source region, ρ the mean far-field density, c the speed of sound in the far-field, and \mathbf{y} a position vector in the source field. Based on this equation, Kraichnan calculated the far-field acoustic power spectral density (Kraichnan 1953)

$$P(\omega) = \pi \frac{\omega^4}{2c^8} \left\langle \left| n_i n_j T_{ij} \left(\frac{\omega \mathbf{n}}{c}, \omega \right) \right|^2 \right\rangle, \quad (2.11)$$

where \mathbf{n} is the unit vector in the direction of the point \mathbf{x} , ω the frequency of the radiated sound, and $T_{ij}(\mathbf{k}, \omega)$ the space-time Fourier transformation of the Lighthill stress tensor.

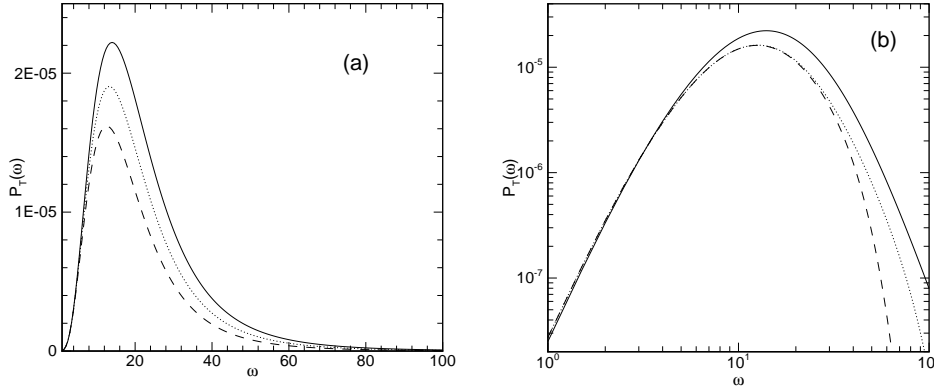


FIGURE 8. Effects of (a) sweeping velocity and (b) unresolved scales on sound power spectra. (a) ——— $V = 1.0$; $V = 0.95$; - - - - $V = 0.90$. (b) ——— $V = 1.0$ with full spectra; $V = 0.95$ and $k_e = 25$; - - - - $V = 0.95$ and $k_e = 13$.

Using the quasi-normal hypothesis, the acoustic power spectral density function can be written in the form (Rubinstein & Zhou 2002)

$$P(\omega) = \frac{\pi}{2} \rho \frac{\omega^4}{c^5} \frac{32\pi}{15} \int_0^{+\infty} 4\pi k^2 \frac{E^2(k)}{(2\pi k^2)^2} dk \frac{1}{2\pi} \int_{-\infty}^{+\infty} R^2(k, \tau) \exp(-i\omega\tau) d\tau \quad (2.12)$$

In the following discussion, the normalized time correlation $R(k, \tau)$ is taken as the exponential form

$$R(k, \tau) = \exp\left(-\frac{1}{2}k^2V^2\tau^2\right). \quad (2.13)$$

and the energy spectrum $E(k)$ assumes the von Kármán form

$$E(k) = C\epsilon^{2/3}k_0^{-5/3}(k/k_0)^4[1 + (k/k_0)^2]^{-17/6}k^{-2}, \quad (2.14)$$

where $k_0 = 5$ defines the peak of energy spectrum. The exponential form and the von Kármán spectrum are the appropriate approximations to the time correlations and the energy spectra, respectively, in our numerical simulations.

With the substitution of (2.13) into (2.12), the non-dimensionalized sound power spectra are given by

$$P_T(\omega) = \frac{2\sqrt{\pi}}{15} \rho M^5 \frac{\omega^4}{V} \int_0^{+\infty} k^{-3} E^2(k) \exp\left(-\frac{\omega^2}{4(Vk)^2}\right) dk, \quad (2.15)$$

where $M = V_0/c$ is the Mach number and $V_0 = \omega_0/k_0$. k_0 is the inverse integral length scale and ω_0 the inverse integral time scale.

The influences of the overpredicted decorrelation scales on acoustic power spectra can be seen in Figure 8(a), where the sound power spectra are evaluated according to (2.15) with the sweeping velocities V equal to 1.0, 0.95 and 0.9. The small variations, up to 10%, of the sweeping velocities cause significant reductions of the sound power spectra at higher frequencies. This illustrates the sensitivity of the acoustic power spectra to the sweeping velocities.

The sweeping velocity induced errors can be compounded by the truncation of the energy spectra at high wavenumbers, corresponding to unresolved scales in LES. To test this effect, the energy spectrum is truncated ($E(k)$ set to zero) for either $k > 25$ or $k > 13$. Figure 8(b) plots the acoustic power spectra for the sweeping velocity $V = 0.95$ with the above truncated energy spectra. It shows that the acoustic power spectra drop considerably at moderate to high frequencies, and the spectral peaks are shifted towards left to lower frequencies.

3. Conclusions and future work

Numerical comparisons in decaying isotropic turbulence suggest that there exist discrepancies in time correlations evaluated by DNS and LES using eddy-viscosity-type SGS models. This is consistent with the previous observations in forced isotropic turbulence. Therefore, forcing is not the main cause of the discrepancies. Comparisons among different SGS models in the LES also indicate that the model choice affects the time correlations in the LES. The multi-scale LES method using the dynamic Smagorinsky model on the small scale equation is the most accurate of the all models, the classic Smagorinsky model is the least accurate and the dynamic Smagorinsky model and spectral eddy viscosity model give intermediate results with small differences.

The generalized sweeping hypothesis implies that time correlations in decaying isotropic turbulence are mainly determined by the instantaneous energy spectra and sweeping velocities. The analysis based on the sweeping hypothesis explains the discrepancies in our numerical simulations: the LES overpredicts the decorrelation time scales because the sweeping velocities are smaller than the DNS values, and underpredicts the magnitudes of time correlations because the energy spectrum levels are lower than the DNS ones. Since the sweeping velocity is determined by the energy spectra, one concludes that an accurate prediction of the instantaneous energy spectra guarantees the accuracy of time correlations.

An analytical expression of sound power spectra based on Lighthill's theory and the quasi-normal closure assumption suggests that the sound power spectra are sensitive to errors in time correlations. Small errors in time correlations can cause significant errors in the sound power spectra, which exhibit a sizable drop at moderate to high frequencies accompanied by a shift of the peaks to lower frequencies.

Based on the above analysis, two possible ways to improve the acoustic power spectrum predictions can be considered. The first is to construct better SGS models to improve the LES accuracy for time correlations. The second is to remedy the temporal statistics of the Lighthill stress tensor in order to "recover" the contribution from the unresolved scales in LES to time correlations.

Acknowledgment: We wish to thank Prof. P. Moin, Dr. A. Wray and Dr. R. Rubinstein for helpful discussions. He's work was partly supported by the National Committee of Science and Technology, P. R. China, under the project "Nonlinear Science".

REFERENCES

- CHOLLET, J.-P. & LESIEUR, M. 1981 Parameterization of small scales of three-dimensional isotropic turbulence utilizing spectral closure. *J. Atmos. Sci.* **38**, 2747–2757.

- CRIGHTON, D. G. 1975 Basic principles of aerodynamic noise generation. *Prog. Aerospace Sci.* **16**, 31-96.
- CRIGHTON, D. G. 1993 Computational aeroacoustics for low Mach number flows. *Computational Aeroacoustics*, ICASE/NASA LaRC Series, edited by J. C. Hardin and M. Y. Hussaini, Springer-Verlag, New York, 50-68.
- GERMANO, M., PIOMELLI, U., MOIN, P. & CABOT, W. H. 1991 A dynamic subgrid-scale eddy viscosity model. *Phys. Fluids A* **3**, 1760-1765.
- HE, G.-W., RUBINSTEIN, R. & WANG, L.-P. 2002 Effects of subgrid scale modeling on time correlations in large eddy simulation. *Phys. Fluids* **14**, 2186-2193.
- HE, G.-W., WANG, M. & LELE, S. K. 2002 Evaluation of subgrid-scale models in terms of time correlations, *Summer Program Proceedings*, Center for Turbulence Research, NASA AmesStanford University, 73-78.
- HUGHES, T. J. R., MAZZEI, L. & OBERAI, A. S. 2001 The multiscale formulation of large eddy simulation: decay of homogeneous isotropic turbulence. *Phys. Fluids* **13**, 505-512.
- KANEDA, Y. & GOTOH, T. 1991 Lagrangian velocity autocorrelation in isotropic turbulence. *Phys. Fluids A* **3**, 1924-1933.
- KANEDA, Y. 1993 Lagrangian and Eulerian time correlations in turbulence. *Phys. Fluids A* **5**, 2835-2845.
- KRAICHNAN, R. H. 1953 The scattering of sound in a turbulent medium. *J. Acoust. Soc. Am.* **25**, 1096-1104
- KRAICHNAN, R. H. 1964 Kolmogorov's hypotheses and Eulerian turbulence theory. *Phys. Fluids* **7**, 1723-1734.
- LIGHTHILL, M. J. 1952 On sound generated aerodynamically: I. General theory. *Proc. R. Soc. Lond.* **A211**, 564-587.
- MENEVEAU, C. & KATZ, J. 2000 Scale-invariance and turbulence models for large eddy simulation. *Annu. Rev. Fluid Mech.* **32**, 1-32.
- PROUDMAN, I. 1952 The generation of sound by isotropic turbulence. *Proc. R. Soc. Lond.* **A214**, 119-132.
- RUBINSTEIN, R. & ZHOU, Y. 2000 The frequency spectrum of sound radiated by isotropic turbulence. *Phys. Lett. A* **267**, 379-383.
- RUBINSTEIN, R. & ZHOU, Y. 2002 Characterization of sound radiation by unresolved scales of motion in computational aeroacoustics. *Eur. J. Mech. B Fluids* **21**, 105-111.
- SEROR, C., SAGAUT, P., BAILLY, C. & JUVÉ, D. 2001 On the radiated noise computed by large-eddy simulation. *Phys. Fluids* **13**, 476-487.
- SMAGORINSKY, J. 1963 General circulation experiments with the primitive equations: I. The basic experiment. *Mon. Weather Rev.* **91**, 99-164.
- WANG, M., LELE, S. K. & MOIN P. 1996 Computation of quadrapole noise using acoustic analogy. *AIAA. J.* **24**, 2247-2254.
- WITKOWSKA, A., JUVÉ, D. & BRASSEUR, J. M. 1997 Numerical study of noise from isotropic turbulence. *J. Comput. Acoust.* **5**, 317-336.